





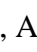



Frequency and Load Effects on Rectifier Bridges and Active Circuits on Mechanical Energy Harvested using Piezoelectric Materials

Youssef El Hmamsy *, Chouaib Ennawaoui **, Oussama Laayati ** Mohamed Aymen Benachour ***, Laadissi El Mehdi *, Loualid El Mehdi *, Ahmed Chebak **, Abdelwahed Hajjaji *

*Laboratory of Engineering Sciences for Energy (LabSIPE), National School of Applied Sciences EL Jadida 24000, Chouaib Doukkali University, Morocco.

**Green Tech Institute (GTI), Mohammed VI Polytechnic University (UM6P), Benguerir 43150, Morocco

***Univ. Polytechnique Hauts-de-France, INSA Hauts-de-France, CERAMATHS – Laboratoire de Matériaux Céramiques et de Mathématiques, F-59313 Valenciennes, France

(elhamsyoussef@gmail.com, chouaib.enna@gmail.com, hajjaji.a@ucd.ac.ma)

‡ Youssef EL HMAMSY; Chouaib Ennawaoui, National School of Applied Sciences EL Jadida 24000, Chouaib Doukkali University, Morocco.

Tel: +212 6 99 919547, elhamsyoussef@gmail.com

Received: 13.10.2022 Accepted: 17.03.2023

Abstract- Today, with the worldwide surge in the price of oil, the energy issue has become an important topic and the possibility of exploiting ambient energy is receiving renewed attention. Thus in this study, we are interested in the devices of recovery of piezoelectric energy of vibration whose final objective is to study the consumption bridge of the diodes and to compare it with the active circuits. The idea is first to extend the life of the battery. Then a second time makes the sensor completely autonomous from an energy point of view.

This work studies the useful characteristics of the diode. For the sake of clarity and under what conditions it can be used, and the characteristic quantities presented by the manufacturer. Each parameter is defined for specific conditions of use. These conditions are specified and correspond to the measurement method used. In addition, this study focuses on power dissipation in diodes in a range of frequencies, and the possibility of replacing the diode bridge with another active circuit as LTC3588-2 and LT4320 in certain conditions consume less energy than diodes. The open circuit tests performed on the transducer allowed us to evaluate the average power recovered at 1.5 mW on an optimal load resistance of 20 K Ω . The signal provided by the transducer was then shaped by simulation. For this, the characteristics of the real diodes of the series 1 N 400X were used, and with the capacitor of 50 μ F, a power of 1.41 mW was obtained on an optimal load resistance of 18.5 K Ω . The management circuit used is a full-wave rectifier in its voltage doubler topology and with the obtained results, its efficiency is evaluated at 35 %.

Keywords Energy harvesting, Piezoelectric, Diode losses, Diode characteristics, Bridge rectifier, Circuit LT4320, Circuit LTC3588-2.

1. Introduction

Presently, the fast growing of technological applications is important in various fields. Which is linked to the efficiency and performance of the components developed. The Schottky diode formed by the metal-semiconductor contact is the most suitable for high frequency applications[1,2]. The technology of semiconductor electronic devices is largely based on metal-semiconductor junctions are components widely used in microelectronics, such as diodes.

A diode is all the more efficient as the reverse voltage that it can support in the state blocked is higher, that its forward voltage drop in the on state is lower and that its switching times are shorter. Since these three conditions cannot be fulfilled simultaneously, the diode must be chosen according to the application for which it is intended [3] .

In this part the diodes are performing according to the conditions of use (frequency, current, voltage...), so the study of the characteristics of each diode is more important to increase the performance and avoid the dissipation of energy in the circuit [4].

Among Special diodes High-voltage diodes, to obtain diodes with high blocking voltage, it is necessary to give the low-doped N⁻ region a large thickness (about 100 μ m per hundreds of volts). This leads to an increase of the forward voltage drop and of the stored charge [5]. On another hand, controlled avalanche diodes, some diodes are designed to withstand the avalanche phenomenon without damage during short but repetitive intervals, the reverse breakdown voltage, the reverse current corresponding to the maximum dissipated power. In addition, fast diodes, these diodes intended to operate at high frequency must have a low residual stored charge Q_R , because the switching losses are proportional to them [6]. To decrease Q_R , it is necessary to reduce the lifetime of the minority carriers in the N⁻ area intending to increase the amount of recombinations during the decay of the forward current. There are also diodes with low forward voltage drops, for example, Schottky diodes. For PN junction diodes, the forward voltage drop is related to the resistivity of the N⁻ zone, which decreases with doping. The epitaxial junction can reduce this voltage drop with precise control of the doping inside each layer. The direct voltage drop for the nominal current can be reduced to less than 1 volt [7,8] .

When a semiconductor, preferably N⁻ type because of the higher electron mobility, is brought into contact with a suitable metal, the thermionic emission of electrons occurs from the metal to the semiconductor and from the semiconductor to the metal. The electrons of the metal are more numerous [9,10]. Still, the semiconductor has more energy and passes into the metal leaving behind them a zone of positive space charge and making an equivalent negative charge appear on the surface of the metal. The positive polarization of the metal with respect to the semiconductor

favors the emission of electrons from the semiconductor towards the metal and a direct current can flow. This current is linked to the voltage V_{AC} by the same relationship as for a PN diode but with a saturation current approximately 5 times higher. Switching is very fast, since the influence of minorities is negligible and there is practically no stored charge [11,12]. At each switching, it is still necessary to inject or extract the charges necessary for the variation of the width of the depletion zone.

Finally, Silicon carbide diodes, several manufacturers offer silicon carbide diodes. This technology is very recent in the recent in the field of power electronics[13,8] . We will give here the advantages of this type of diodes.

- Direct voltage comparable to Schottky diodes.
- No influence of the temperature on the switching characteristics.
- No overvoltage on closing.
- No overlapping load.
- Thermal resistance 3 to 5 times lower than for an ultrafast silicon diode.

In this work, we first presented the electrical properties of the different diodes, also presented comparison between the Schottky barrier and the classic PN junction diode intending to better be understanding the Schottky diode. Then we have studied a mechanical energy recovery system. In practice, these systems recover the little energy (rectifier bridge circuit LTC3588-2, and LT4320 circuit) from ambient vibrations intending to supply low consumption electrical systems (typically a few μ W to mW) [14–16] . In addition was to realize rectification circuits for the recovery of piezoelectric energy, it was firstly a question of choosing the diode as well as the topology of rectifier the most appropriate for the design of the circuits. Using the equivalent small signal model of a Schottky diode, it was obtained through simulations on LtSpice that the diodes (BAT41, 1N4001, 1N4148, BAT54s, 1N5817), and the integrated circuits (LTC3588-2, LT4320) is the one that offers the best performance in terms of conversion efficiency.

The aim of this work is to calculate the power dissipated in a diode (Section 2). In Section 3, the authors present the diode using in simulation part. Section 4 studied the simulation of the different rectifier bridges, then search for the power maximization point. Hence, in the Section 5 study of the effect of some parameters (load, frequency) with the efficiency of each circuit, experimental results in the section 6, Finally (Section 7) conclusions from this work.

2. Diode losses analysis

2.1. The recovered charge characteristics

When the junction is directly polarized, the external electric field opposes the internal electric field created by the ions stripped of their free electron (N zone) or hole (P zone), thus allowing a greater diffusion of the majority carriers in the region of the opposite type where they become a minority. They then recombine with a charge of the opposite sign [17,18]. The recombination phenomenon is not instantaneous, the carriers have a lifetime t equal to about 1ms in silicon. If we reverse the polarity abruptly at the terminals of the diode intending to block it, these carriers will behave in the same way as the minority carriers in the established reverse regime they will form an intense current that will be added to the leakage current I_s , until the stored charge disappears. This current will decrease until it becomes zero for a time t_{RR} (Reverse Recovery Time).

2.2. Calculation of diode losses

To determine the dissipation, it is necessary to know the types of power (losses) dissipated in the component.

2.2.1 Conduction Loss

When a diode is suddenly reverse-biased after a period of conduction, charges have accumulated in the forward junction. The diode then takes some time to regain its blocking power and evacuate the excess charge, this is called the reverse recovery phase [19–21]. For normal values of the direct current, in a given operating point, the instantaneous power P_c dissipated in the diode is:

➤ *Conduction Loss P_c (on)*

The diode can be represented with the aid of a barrier workable in series with a low ahead resistance R_0 . Therefore, the diode’s on-state loss occurred when a massive ahead contemporary I_F is flown in the circuit.

$$P_{on} = V_0 \times \bar{I}_F + R_0 \times I_F^2$$

Since the value of R_0 is very small, the on-state loss of the diode is primarily determined by the barrier potential V_0 . A low barrier potential is essential to minimize the on-state loss of the diode.

➤ *Conduction Loss P_r (off) (P_r usually negligible)*

The leakage current in the blocked state is very low, the losses in the blocked state, equal to the product of this current and the reverse voltage applied to the diode, are generally negligible compared to the losses in the conducting state.

2.2.2 Switching loss

Switching on closing (switching ON) corresponds to the passage from the blocked state to the on state, switching on opening (switching OFF) to the reverse passage, with static characteristics, these changes of the state depend on both the semiconductor component and the circuit in which it is inserted [22–24].

➤ *Turn-on losses (P_{on})*

When switch Q is closed, the current from a source I flows into the voltage source U, which imposes a voltage $V_F = -U$ across the diode [25]. When the switch Q is opened (figure 1. (a)), the capacitor C charges at constant current I, at the instant $t = 0$, the negative voltage V_F becomes positive. In addition, the forward current begins to flow, the voltage drop decreases and tends towards its equilibrium value V_F (Figure 1 (b)).

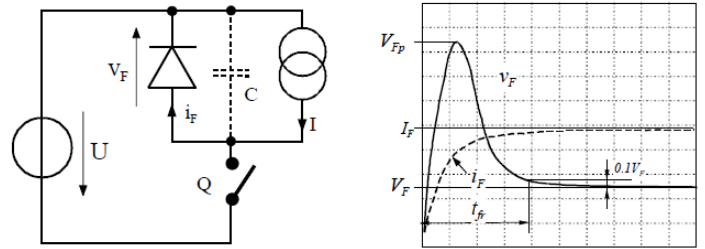


Fig. 1. Current and voltage curve during switching on

closing [25]

For switching on closing, the behavior of a diode characterized by:

The peak forward voltage V_{FP} or V_{FM} (peak forward voltage), maximum value of V_F during switching. These parameters depend on the applied current, its speed of establishment and the temperature.

$$P_{on} = \frac{1}{2} \times t_{fr} \times V_{FP} \times \hat{I}_F \times f$$

Where:

t_{FR} : Forward recovery time

f : Operating frequency

➤ *Turn-off losses (P_{off})*

The switching of the diode at the opening (Figure 2 (a)) gives the equivalent diagram. The current source I gives the current to be switched off, the voltage source U gives the reverse voltage after opening (Figure 2 (b)).

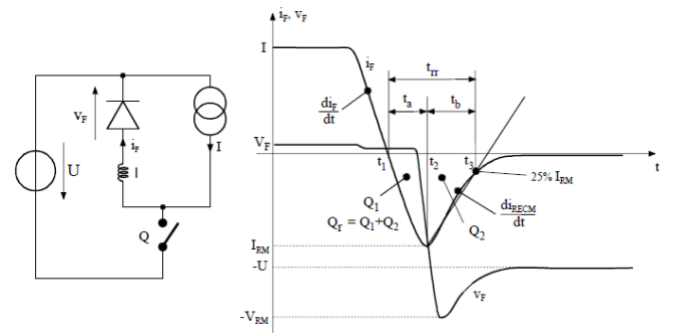


Fig. 2. Current and voltage curve during switching on

opening [25]

$$P_{off} = \frac{1}{4} \times V_R \times I_{RM} \times t_{rr} \times f = \frac{1}{2} \times V_R \times Q_{rr} \times f$$

$$Q_{rr} = \frac{1}{2} \times I_{RM} \times t_{rr}$$

At the time of blocking, the evacuation of the stored charge Q_1 leads to the recovery phenomenon illustrated in Figure 2. A slight reverse current appears up to the value $-I_{RM}$ during the recovery time t_r . Then the diode replenishes its potential barrier by gaining the Q_2 load which causes a slight negative overvoltage $-V_{RM}$. This voltage lasts until the current is removed, then returns to $-U$, the voltage delivered by the power source.

Power loss P_t is the total of all these values.

$$P_t = P_{c(on)} + P_{on} + P_{off} + P_r \quad [W]$$

The process described above leads to the dissipation of a recovery power P_r in switching which depends on the charges passing through Q , the source voltage U and the switching frequency f .

Table 1. The characteristics of the diodes [26,27]

Diode	BAT54s	1N5711	1N5817	BAT41	1N4148	1N4001
type	Schottky	Schottky	Schottky	Schottky	Silicon	Silicon
Repetitive peak reverse voltage V_{RR}	30V	70V	20V	100V	100V	50V
Forward	0.41V @10mA	0.41V @1mA	0.45V @1A	0.45V @1mA	1V@10mA	1.1V @1A
Voltage drop(25°C)	2µA@25V	0.2µA@50V	12 µA @20V	100nA@50 V	25 nA @20V	5µA@50V
Forward Continuous current(25°C)	200 mA	15mA	1A	100mA	300mA	1A
t_{RR}	5nA	1ns	10ns	5ns	4ns	30µs

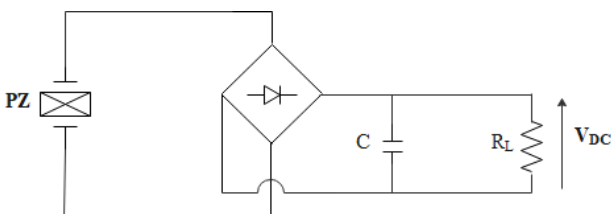
These data are insufficient for the final selection of a component. The description is more marketing than technical, but with a little practice, it is possible to define the category to which the component belongs and to make a quick comparison with other manufacturers.

4. Simulation model

In this part, we have studied the performance of six types of rectifier bridge for harvesting energy delivered by the piezoelectric, and we will also compare it with other LT4320 and LTC3588 circuits, the Ltspice software being used in the simulation study

4.1. Bridge rectifier

Energy harvested from a vibration, the signal delivered by the piezoelectric is therefore alternating. The simplest way to recover all the energy is to use a bridge rectifier and store the energy in a capacitor C_{pz} .



3. Diode characteristics

In the following sections, we will cover the useful characteristics of the diode. Manufacturers each have their own way of presenting the characteristics of their components. For reasons of clarity, each parameter is defined for specific conditions of use. These conditions are specified and correspond to the measurement method used. Therefore, necessary to be careful when analysing a particular problem.

In the power supply of the amplifiers, there are classic rectifier diodes such as the 1N4001 diode with a voltage drop of about 50 V, it is possible to find another category of diodes with a lower voltage drop. These are Schottky diodes, an example BAT54s and 1N5711.

Fig. 3. The bridge rectifier circuit

In this part, we have studied the bridge rectifier circuit making it possible to recover the energy delivered by the piezoelectric (Figure 3). Where $I = 566 \mu A$ of frequency $F = 100 \text{ Hz}$, and the filter capacitor is $50 \mu F$. Using the LtSpice software, we simulate the bridge rectifier circuit for 1s, and also circuits LT4320, LTC3588-2. All the used parameters are given in the Table 2 below [28,31].

Table 2. The values of the used components

Parameter	Value/model
I_{pz}	566 µA
C_{pz}	75 nF
F	100 Hz
C	50 µF
Diode	1N5817/BAT41/1N4148/1N5711/BAT54SSs/1N4001

4.2. Circuit LT4320

The LT4320 devices are ideal diode bridge controllers that drive four N-channel MOSFETs, supporting voltage rectification from DC to 600 Hz. By optimizing available voltage and reducing power dissipation, the ideal diode bridge simplifies power supply design and reduces power supply costs, especially in low voltage applications [32].

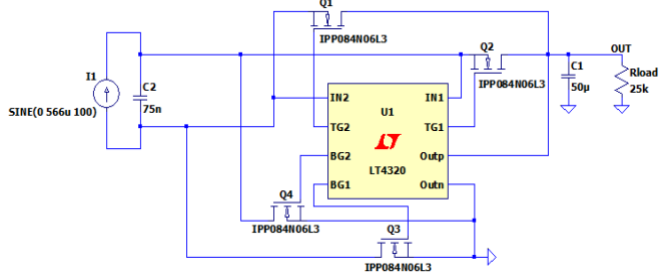


Fig. 4. Simulation model of the circuit LT4320 by LtSpice

An ideal diode bridge also eliminates thermal design issues and expensive heat sinks, and significantly reduces IC board area. The LT4320's internal charge pump supports full NMOS designs, eliminating larger and more expensive PMOS switches. In the event of a power source failure or short circuit, a quick shutdown minimizes reverse current transients.

4.3. Circuit LTC3588-2

The model LTC 3588-2 (Figure 5) integrates a low-loss full-wave rectifier bridge with a high-efficiency step-down converter to form a full energy recovery solution optimized for high-output impedance power sources as piezoelectric, solar or magnetic transducers [33–35].

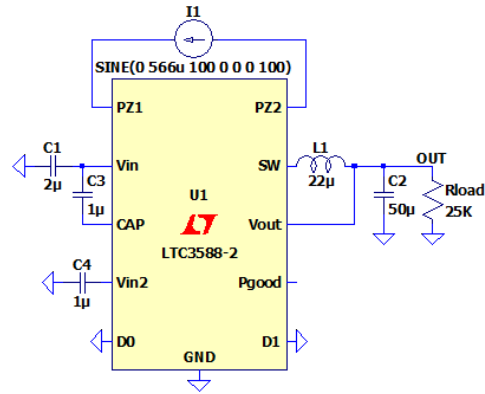


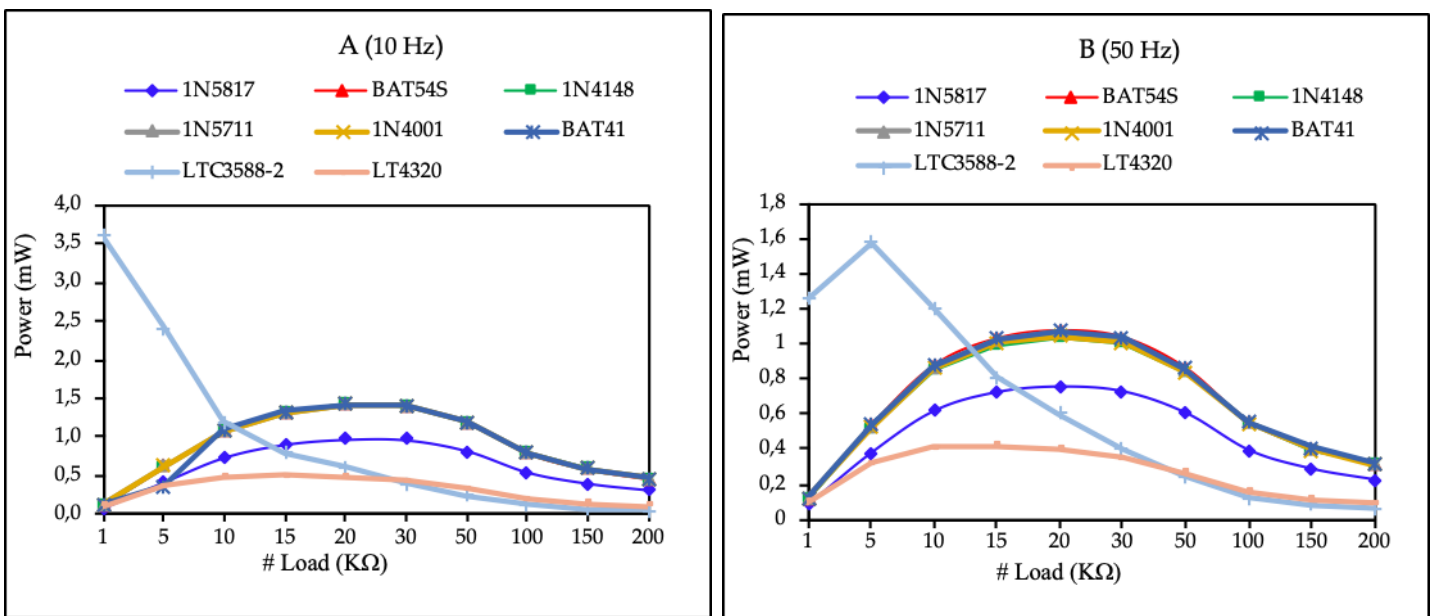
Fig. 5. Simulation model of the circuit LTC3588-2 by LtSpice

An ultra-low standby current undervoltage lockout mode (UVLO) allows efficient extraction of energy from sources with high open-circuit voltages. This energy is transferred from the input capacitor to the output via a high-efficiency synchronous step-down regulator.

5. Simulation results

5.1. Load influence on harvested power

The objective in this part is to find the performance point of each bridge rectifier studied, Figure 6 shows the power variation as a function of load, we have changed the resistance to find the point of maximum power. The simulation is repeated for several resistance values between 1kΩ and 200kΩ. With a capacity of 50 μF, and constant source frequency.



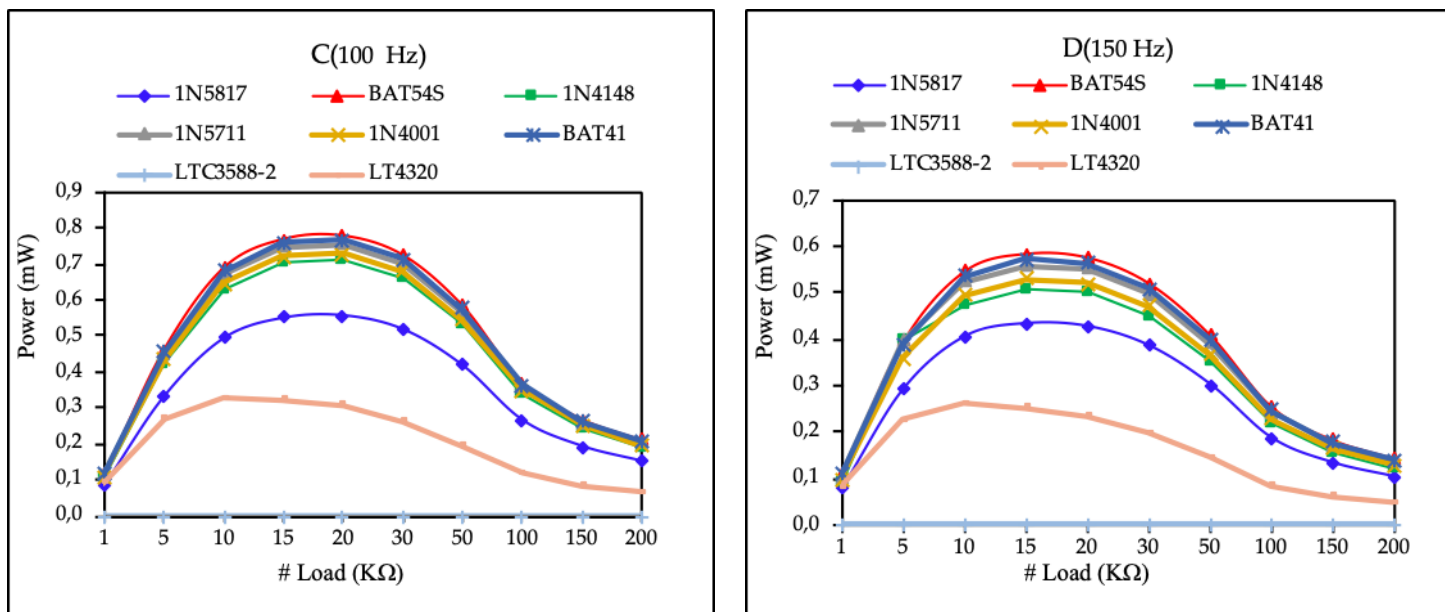


Fig.6. Power variations as a function of the load

The LTC3588-2 circuit extracts more energy in curve (A) and curve (B), sometimes more than 70 %. While in the other circuits the rate of extraction of energy is quite close so that we can see that the BAT54SS diode BAT41 and 1N5711 are slightly better than 1N5817 and 1N4001, as the power rises between 5kΩ and 100kΩ and is almost maximum at 15kΩ. With a higher load, the power begins to decrease, then that the power is almost constant at the rate of the LT4320 circuit at 50Hz and 10Hz. In addition, for curve (C) and curve (D), we find that the power of the LTC3588-2 circuit is very low and that the power of the LT4320 is almost constant in both cases. Regarding the circuit formed by the diode, we find a maximum power between 5kΩ and 100kΩ with a slight increase in the circuit BAT54SS and 1N5711.

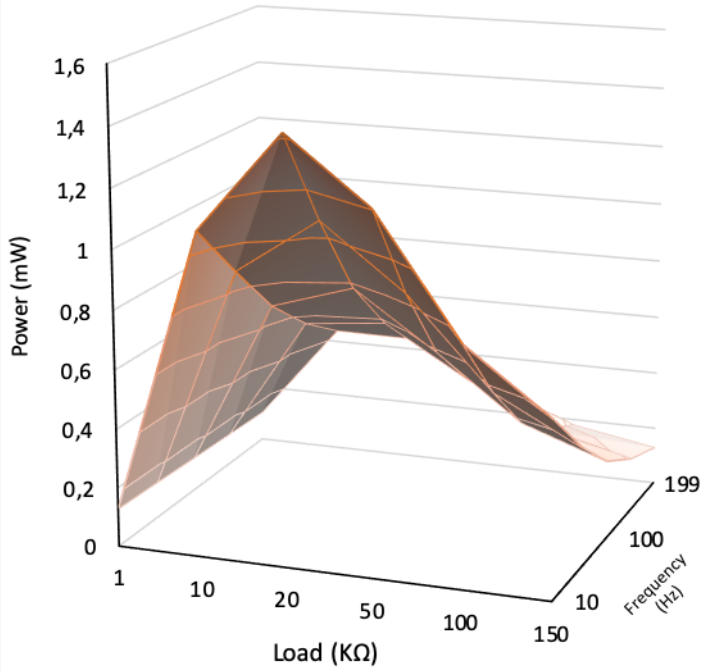
5.2. The power as a function of frequency and load

To investigate the various diode rectifiers, we started by assuming the source of the AC voltages to be perfect (zero impedance) and the current receiver to be highly inductive leading to a constant current. Then, to correct the results obtained by evaluating the voltage drop on load, we took into account the impedance of the source while still assuming the rectifier to be strongly inductive.

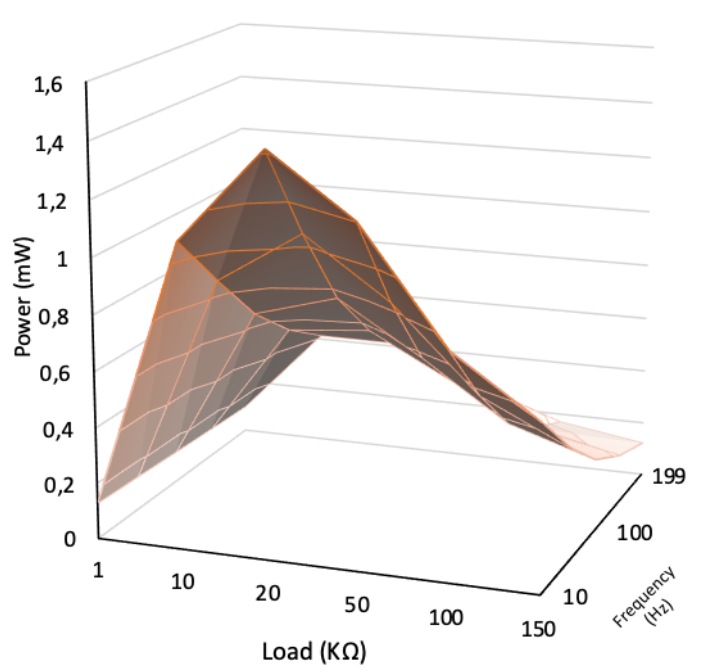
To complete this study of diode rectifiers, we have examine the influence of the nature of the receiver on the operation of the circuits and the value of the various variables, intending to see to what extent it is necessary to correct the results obtained by assuming the receiver to be strongly inductive.

Figure 7 gives the maximum values of each circuit and specifies the maximum power coordinates.

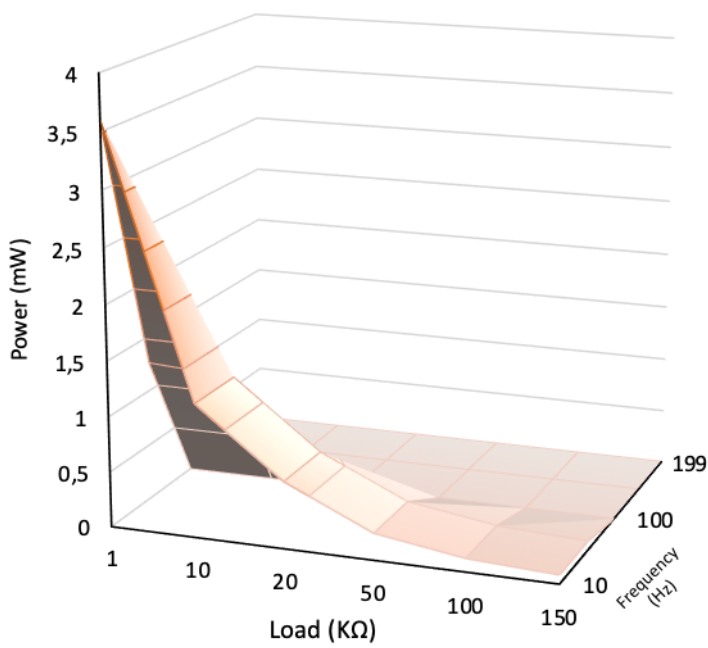
A(BAT54s)



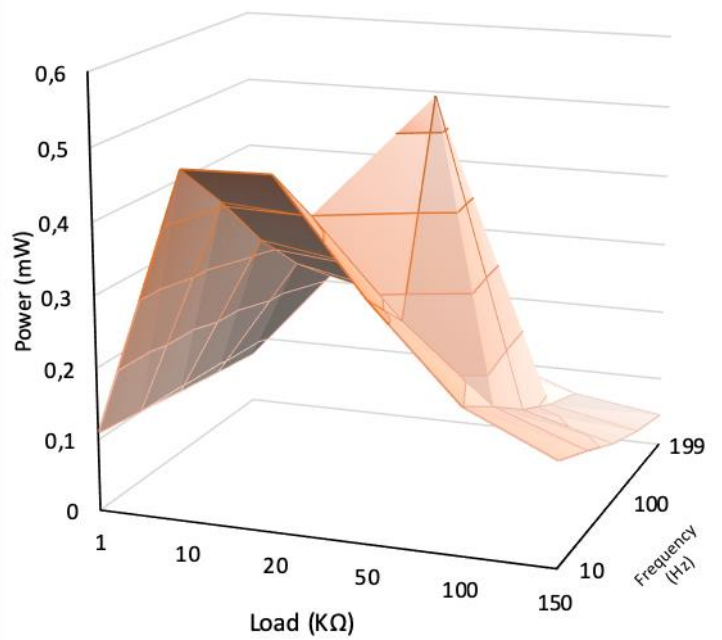
B(1N5711)



C(LTC3588-2)



D(LT4320)



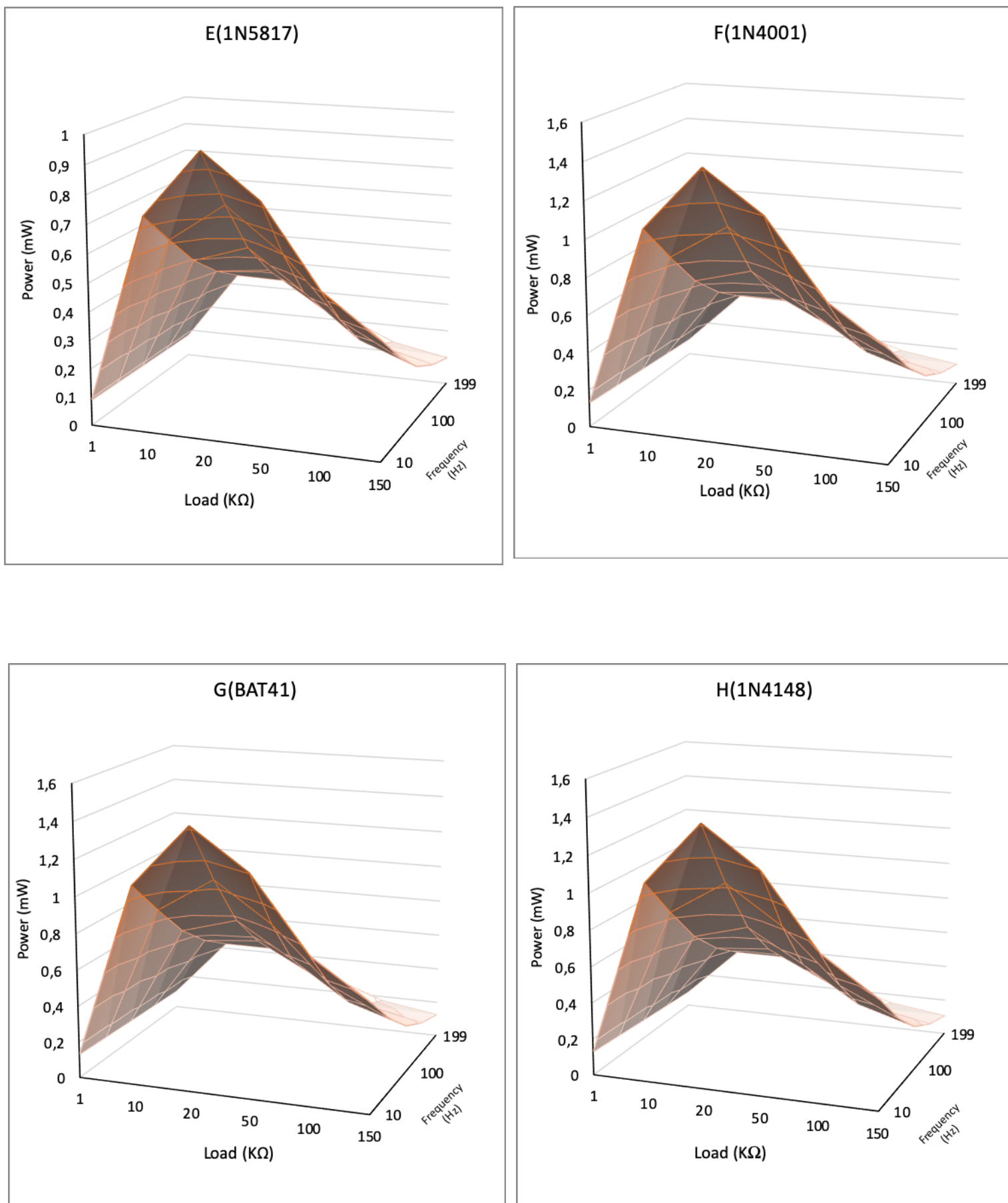


Fig. 7. Power variation as a function of load and frequency

The curve (A) of diodes BAT54S and curve (B) 1N5711 came after having noted the previous results, as well as the difference between the Schottky diode and the conventional diode. Through these results, the power varies depending on the load and the frequency generated. The LTC3588-2 circuit (curve C) has good performance at a frequency lower than 50Hz, while above 50Hz the power is very low. As for the LT4320 circuit (curve D), the power is almost constant and it is at the maximum 10kΩ and 20kΩ in all the frequencies studied. On the other hand, the power of bridge rectifier is maximum at the frequencies of 10Hz and 20Hz, It begins to decrease as the frequency increases, this change is explained by the switching phenomenon The higher the frequency, the

more energy dissipated in the diode, in addition to the energy dissipated by conduction. For the curves E, F, G and H for the rectifier bridges respectively (1N5817), (1N4001), (BAT41) and (1N4148) the almost maximum power in the point (F=10 Hz, R= 20 KΩ). From the input power (Pin) and output power (Pout) we will calculate the dissipated power (Pds) and the gain G of each rectifier bridge.

All the used parameters are given in the table 3 below (Frequency f and load R).

Table 3. The coordinates of maximum power

	R (KΩ)	F (Hz)	Pin (mW)	Pout (mW)	Pds (mW)	G
1N5817	20	10	1,60	9,74	6,23	61%
LTC3588-2	1	10	4,92	3,60	1,31	73%
LT4320	50	100	1,05	5,46	5,02	52%
1N4001	20	10	2,14	1,41	7,32	66%
BAT54	20	10	2,00	1,42	5,74	71%
1N5711	20	10	2,09	1,42	6,70	68%
1N4148	20	10	2,18	1,41	7,73	65%

By using the various characteristics given in curves by the manufacturer, it is possible to determine the conduction and switching losses for a given operating point.

reverse current does not affect the input/output characteristic of the converter and the diode can be considered ideal when switching from open to closed state.

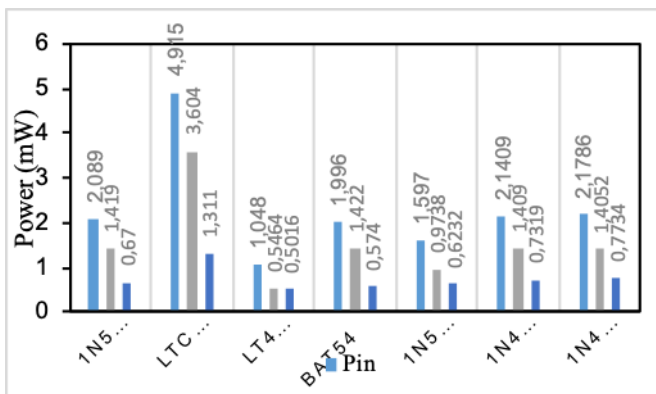


Fig.8. Power variations as a function of frequency

According to the figure 8, the lost power is absorbed between 27% and 48% depending on the circuit, due to the phenomenon of switching and conduction. The maximum recovery current I_{RM} can sometimes induce over voltages in inductive circuits. Notwithstanding, in many circuits, this

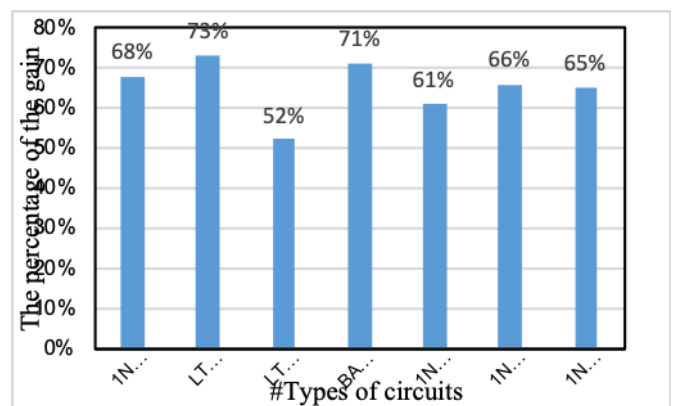


Fig. 9: Gain of output power

Figure 9 represents the percentage of each component in the performance points (f, R), the performance of the LTC 3588-2 circuit is good at (f = 10Hz, R = 1kΩ), with a diode ratio close to the maximum power at the same coordinates (f

= 10Hz, R = 10 kΩ), the peak power for the LT4320 circuit (f = 100Hz, R = 50 kΩ).

The reverse saturation current density of the Schottky junction is orders of magnitude greater than that of the ideal PN diode. Recall that the saturation current in a silicon PN junction is dominated by the current generation. A typical generation current density is about $10^{-7} \text{A} / \text{cm}^2$, which is always 2-3 times lower than the saturation of the Schottky diode.

6. Experimental Results

The objective of this part of the research is to realize piezoelectric energy harvesting systems. For this, the rectifier bridges (Figure 10) have been studied to receive the signals and the rectifier circuits have been optimized for incident power. Circuits can be characterized by their conversion efficiency, which describes the ability of the rectifier to provide continuous electrical power to the load from piezoelectric energy.

To validate the performance of the different rectifier bridges, the experiment was carried out on a prototype which contains a piezoelectric generator. Figure 11 represents the model of this generator. It is a generator of based on material the piezoelectric transducers PZ1 88 where the thickness of each piezoelectric layer is 0.35mm

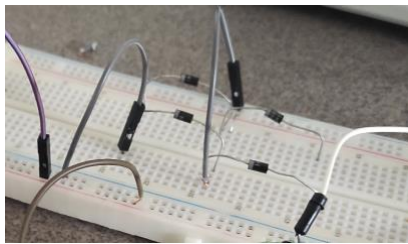


Fig.10. Bridge rectifier

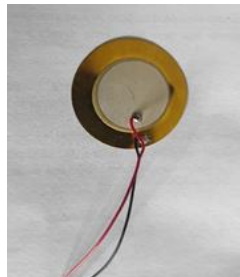


Fig.11. Piezoelement

The piezoelectric element PZ1 88 connected to a vibrating generator which generates an excitation to simulate the vibration environment. Figure 12 represents the experimental setup used, the characteristics of which are in Table 4.

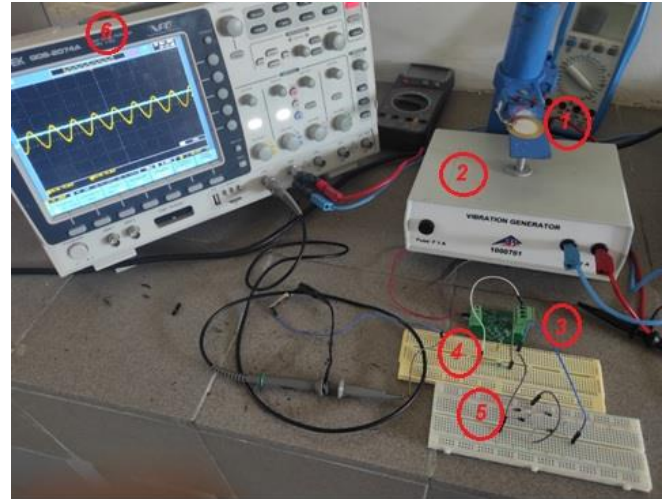


Fig. 12. Experimental set up

To show the validity of the proposed model for the piezoelectric generator. Then we measured the voltage at the output of the generator for several values of load resistance R_{load} . Based on the proposed model presented in the simulation chapter, we obtain the formula for the generator voltage as a function of the other model parameters. The excitation consists of a force applied to the end of the beam and the piezoelectric voltage is measured at the transducer electrodes. Table 4 shows that the image above is composed by:

Table 4. Parameters of the experimental system.

Components/Parameters	Type/Values
1) Piezoelectric element	PZ1 88, 35 mm
2) Cantilever beam	300*20*2 mm
3) Interface circuit.	LTC3588-2/ LT4320
4) Inductors for voltage inversion.	2.2 mH
5) Bridge Rectifier	BAT54s/1N5817/ BAT41/ 1N4001/1N4148
6) Digital oscilloscope for visualization	
7) Applied frequency f	100 Hz
8) Load capacitors, C_L	50 μF
9) Load resistors, R_L	5 K Ω , 10 K Ω , 20 K Ω

In this part compares the power frequency sweep response of each bridge rectifier model proposed in the simulation part with that obtained experimentally.

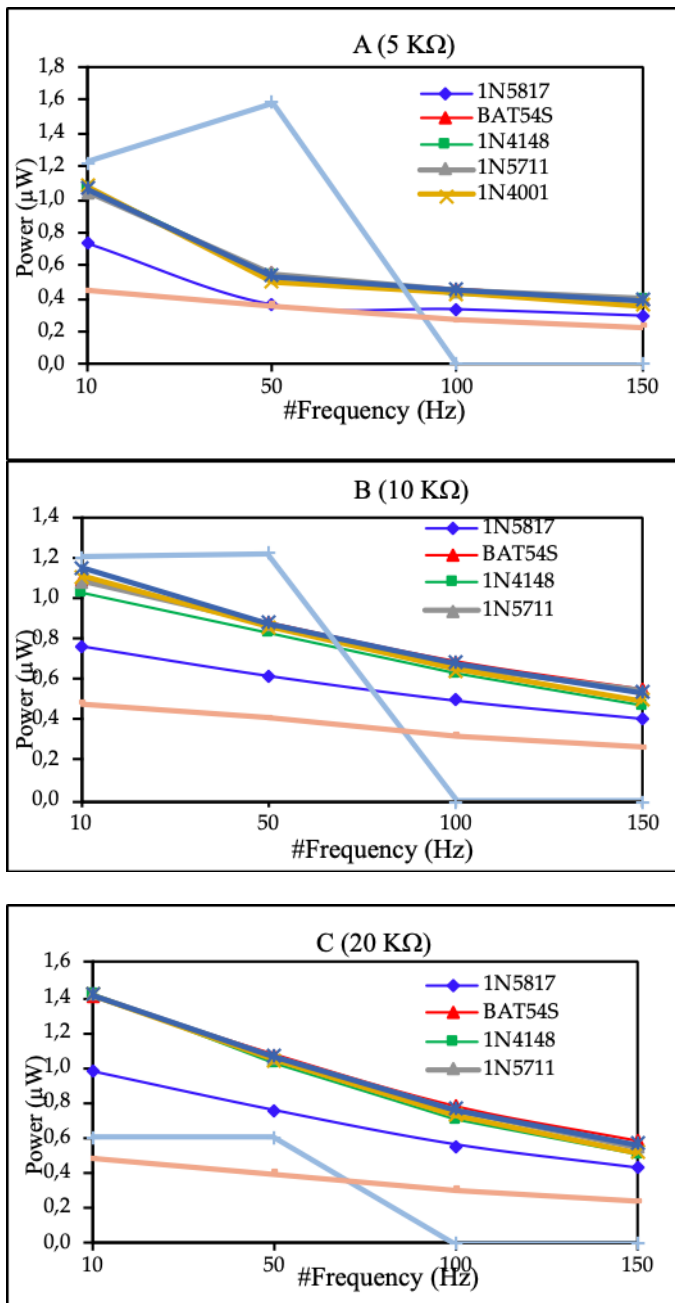


Fig. 13. The real power experimental measurements for the different bridge rectifiers as a function of the frequency for three different load values: 5KΩ, 10KΩ and 20KΩ.

The experimental measurements are carried out in the same band of frequency of sweep (10 Hz, 150 Hz). Figure 13 shows that when the frequency is less than or equal to 50 Hz, the response of the LTC3588 circuit is important compared to the other models for curve A ($R=5\text{ K}\Omega$) and curve B ($R=10\text{ K}\Omega$) and very close to the real response. The rectifier bridges (BAT41, 1N4001, 1N4148, BAT54s) show almost the same result with a decrease when the frequency increases $P_{out}(\text{max})=1.07\mu\text{W}$, $P_{out}(\text{max})=1.2\mu\text{W}$, $P_{out}(\text{max})=1.42\mu\text{W}$ respectively 5 KΩ, 10 KΩ, 15 KΩ. The advantage of the LTC3588 circuit is not affected $P_{out}(\text{max})=0.48\mu\text{W}$ despite

the change in frequency but the efficiency remains low compared to the other circuits.

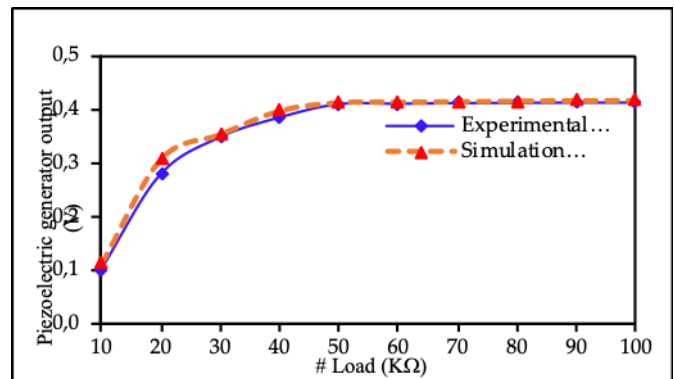


Fig. 14. Comparison between experimental and analytical results ($f=35\text{ Hz}$)

On figures 14, we observe a good agreement between the experimental results and those resulting from the simulations with conversion efficiencies reaching 30% with a DC voltage of 0.42 V at 50 KΩ. The conversion efficiencies reaching 40% in the case of simulations and 20% in experimental measurements. This can be explained by the fact that the losses attributable to the transmission lines, which are inversely proportional to the square of the frequency at 35 Hz.

7. Conclusion

The open circuit tests performed on the transducer allowed to evaluate the average power recovered at 1.5 mW on an optimal load resistance of 20 KΩ. The signal provided by the transducer was then shaped by simulation. For this, the characteristics of the real diodes of the series 1 N 400X were used, and with capacitor of 50 µF, a power of 1.41 mW was obtained on an optimal load resistance of 18.5 KΩ. The management circuit used is a full-wave rectifier in its voltage doubler topology and with the obtained results, its efficiency is evaluated at 73%.

The extraction of energy from weak energy sources such as piezoelectric sources depends on circuits made up of diodes, or other circuits such as LTC3588-2 and LT4320. In this work, we study each circuit and its cost-effectiveness by load and the frequency of the source (piezoelectric element), if this study enables us to choose the appropriate circuit to extract maximum power and avoid its dissipation.

Finally, another view of this high-frequency use is the internal capacitance, a Schottky diode has no diffusion capacitance since there are no minority carrier diffusion currents. The capacitance's overall is lower, so the cutoff frequency is higher. Notwithstanding, Schottky diodes have other characteristics a high reverse saturation current and a threshold voltage generally lower than a conventional PN diode. Their use in low frequency is not advantageous.

References

- [1] M. Lallart, L. Garbuio, L. Petit, C. Richard, D. Guyomar, Double synchronized switch harvesting (DSSH): a new energy harvesting scheme for efficient energy extraction, *IEEE Trans. Ultrason. Ferroelectr. Freq. Control.* 55 (2008) 2119–2130. <https://doi.org/10.1109/TUFFC.912>. (Article)
- [2] M. Yuan, Z. Cao, J. Luo, Characterization the influences of diodes to piezoelectric energy harvester, *Int. J. Smart Nano Mater.* 9 (2018) 151–166. <https://doi.org/10.1080/19475411.2018.1454532>. (Article)
- [3] A. Taya, Sofyan., and Malek G. Daher. "Properties of defect modes of one-dimensional quaternary defective photonic crystal nanostructure." *International Journal of Smart Grid-ijSmartGrid* 6.2 (2022): 30-39. <https://doi.org/10.20508/ijsmartgrid.v6i2>. (Article)
- [4] C. Ennawaoui, H. Lifi, A. Hajjaji, A. Elballouti, S. Laasri, A. Azim, Mathematical modeling of mass spring's system: Hybrid speed bumps application for mechanical energy harvesting, *Eng. Solid Mech.* (2019) 47–58. <https://doi.org/10.5267/j.esm.2018.11.002>. (Article)
- [5] M.B. Khan, D.H. Kim, J.H. Han, H. Saif, H. Lee, Y. Lee, M. Kim, E. Jang, S.K. Hong, D.J. Joe, T.-I. Lee, T.-S. Kim, K.J. Lee, Y. Lee, Performance improvement of flexible piezoelectric energy harvester for irregular human motion with energy extraction enhancement circuit, *Nano Energy.* 58 (2019) 211–219. <https://doi.org/10.1016/j.nanoen.2019.01.049>. (Article)
- [6] A. Hajjaji, D. Guyomar, S. Touhtouh, S. Pruvost, Y. Boughaleb, M. Rguiti, C. Courtois, A. Leriche, K. Benkhouja, Nonlinearity and scaling behavior in a soft lead zirconate titanate piezoceramic, *J. Appl. Phys.* 108 (2010) 064103. <https://doi.org/10.1063/1.3486510>. (Article)
- [7] C. Ennawaoui, H. Lifi, A. Hajjaji, C. Samuel, M. Rguiti, S. Touhtouh, A. Azim, C. Courtois, Dielectric and mechanical optimization properties of porous poly(ethylene-co-vinyl acetate) copolymer films for pseudo-piezoelectric effect, *Polym. Eng. Sci.* 59 (2019) 1455–1461. <https://doi.org/10.1002/pen.25132>. (Article)
- [8] M. Lallart, G. Lombardi, Synchronized Switch Harvesting on ElectroMagnetic System: a nonlinear technique for hybrid energy harvesting based on active inductance, *Energy Convers. Manag.* 203 (2020) 112135. <https://doi.org/10.1016/j.enconman.2019.112135>. (Article)
- [9] G. Shi, J. Chen, Y. Peng, M. Shi, H. Xia, X. Wang, Y. Ye, Y. Xia, A Piezo-Electromagnetic Coupling Multi-Directional Vibration Energy Harvester Based on Frequency Up-Conversion Technique, *Micromachines.* 11 (2020) 80. <https://doi.org/10.3390/mi11010080>. (Article)
- [10] A. Brenes, A. Morel, J. Juillard, E. Lefevre, A. Badel, Maximum power point of piezoelectric energy harvesters: a review of optimality condition for electrical tuning, *Smart Mater. Struct.* 29 (2020) 033001. <https://doi.org/10.1088/1361-665X/ab6484>. (Article)
- [11] M. Rajarathinam, S.F. Ali, Energy generation in a hybrid harvester under harmonic excitation, *Energy Convers. Manag.* 155 (2018) 10–19. <https://doi.org/10.1016/j.enconman.2017.10.054>. (Article)
- [12] M. Lallart, W.-J. Wu, L. Yan, S.-W. Hung, Inductorless Synchronized Switch Harvesting Using a Piezoelectric Oscillator, *IEEE Trans. Power Electron.* 35 (2020) 2585–2594. <https://doi.org/10.1109/TPEL.2019.2925709>. (Article)
- [13] A. Brenes, A. Morel, J. Juillard, E. Lefevre, A. Badel, Maximum power point of piezoelectric energy harvesters: a review of optimality condition for electrical tuning, *Smart Mater. Struct.* 29 (2020) 033001. <https://doi.org/10.1088/1361-665X/ab6484>. (Article)
- [14] L. Wu, P. Zhu, M. Xie, A Self-Powered Hybrid SSHI Circuit with a Wide Operation Range for Piezoelectric Energy Harvesting, *Sensors.* 21 (2021) 615. <https://doi.org/10.3390/s21020615>. (Article)
- [15] Y.E. Hmamsy, C. Ennawaoui, A. Hajjaji, Topology network effects for DSSH circuit on vibration energy harvesting using piezoelectric materials, *Indones. J. Electr. Eng. Comput. Sci.* 25 (2022) 721. <https://doi.org/10.11591/ijeecs.v25.i2.pp721-731>. (Article)
- [16] A. Hajjaji, D. Guyomar, S. Pruvost, S. Touhtouh, K. Yuse, Y. Boughaleb, Temperature/electric field scaling in Ferroelectrics, *Phys. B Condens. Matter.* 405 (2010) 2757–2761. <https://doi.org/10.1016/j.physb.2010.03.023>. (Article)
- [17] C. Ennawaoui, A. Hajjaji, C. Samuel, E. Sabani, A. Rjafallah, I. Najihi, E.M. Laadissi, E.M. Loualid, M. Rguiti, A.E. Ballouti, A. Azim, Piezoelectric and Electromechanical Characteristics of Porous Poly(Ethylene-co-Vinyl Acetate) Copolymer Films for Smart Sensors and Mechanical Energy Harvesting Applications, *Appl. Syst. Innov.* 4 (2021) 57. <https://doi.org/10.3390/asi4030057>. (Article)
- [18] Y.E. Hmamsy, C. Ennawaoui, E.M. Loualid, E.M. Laadissi, A. Balhamri, A. Hajjaji, Mathematical model of Mono-DSSH network topology of energy harvesting optimization, in: 2022 11th Int. Symp. Signal Image Video Commun. ISIVC, IEEE, El Jadida, Morocco, 2022: pp. 1–5. <https://doi.org/10.1109/ISIVC54825.2022.9800215>. (Conference Paper)
- [19] MHK. Khan, and M. A. A. Rakib. "Implementation of Inverse Define Minimum Time Under and Over Voltage Relay." *International Journal of Smart Grid-ijSmartGrid* 5.2 (2021): 88-93. <https://doi.org/10.20508/ijsmartgrid.v5i2>. (Article)
- [20] Y. El Hmamsy, C. Ennawaoui, E.M. Laadissi, E.M. Loualid, A. Hajjaji, Optimized piezoelectric energy harvesting circuit using DC/DC converter, *Mater. Today Proc.* 66 (2022) 473–478. <https://doi.org/10.1016/j.matpr.2022.07.219>. (Article)

- [21] A. AlKassem, M. Al Ahmadi, and A. Draou. "Modeling and simulation analysis of a hybrid PV-wind renewable energy sources for a micro-grid application." 2021 9th International Conference on Smart Grid (icSmartGrid). IEEE, 2021. <https://doi.org/10.1109/icSmartGrid52357.2021.9551215>. (Article)
- [22] M. Balato, L. Costanzo, A. Lo Schiavo, M. Vitelli, Optimization of both Perturb & Observe and Open Circuit Voltage MPPT Techniques for Resonant Piezoelectric Vibration Harvesters feeding bridge rectifiers, *Sens. Actuators Phys.* 278 (2018) 85–97. <https://doi.org/10.1016/j.sna.2018.05.017>. (Article)
- [23] L. Costanzo, Alessandro Lo Schiavo, and Massimo Vitelli. "Design guidelines for the perturb and observe technique for electromagnetic vibration energy harvesters feeding bridge rectifiers." *IEEE Transactions on Industry Applications* 55.5 (2019): 5089–5098. <https://doi.org/10.1109/TIA.2019.2923162>. (Article)
- [24] C. Ennawaoui, A. Hajjaji, A. Azim, Y. Boughaleb, Theoretical modeling of power harvested by piezo-cellular polymers, *Mol. Cryst. Liq. Cryst.* 628 (2016) 49–54. <https://doi.org/10.1080/15421406.2015.1137679>. (Article)
- [25] M. Edla, Y.Y. Lim, M. Deguchi, R.V. Padilla, I. Izadgoshasb, An Improved Self-Powered H-Bridge Circuit for Voltage Rectification of Piezoelectric Energy Harvesting System, *IEEE J. Electron Devices Soc.* 8 (2020) 1050–1062. <https://doi.org/10.1109/JEDS.2020.3025554>. (Article)
- [26] Alldatasheet, (n.d.). <https://www.alldatasheet.com/> (accessed September 13, 2022).
- [27] J. Sadecki, W. Marszalek, Complex oscillations and two-parameter bifurcations of a memristive circuit with diode bridge rectifier, *Microelectron. J.* 93 (2019) 104636. <https://doi.org/10.1016/j.mejo.2019.104636>. (Article)
- [28] A. Erturk, D.J. Inman, Issues in mathematical modeling of piezoelectric energy harvesters, *Smart Mater. Struct.* 17 (2008) 065016. <https://doi.org/10.1088/0964-1726/17/6/065016>. (Article)
- [29] F. Qian, T.-B. Xu, L. Zuo, Design, optimization, modeling and testing of a piezoelectric footwear energy harvester, *Energy Convers. Manag.* 171 (2018) 1352–1364. <https://doi.org/10.1016/j.enconman.2018.06.069>. (Article)
- [30] J. Wang, Z. Shi, H. Xiang, G. Song, Modeling on energy harvesting from a railway system using piezoelectric transducers, *Smart Mater. Struct.* 24 (2015) 105017. <https://doi.org/10.1088/0964-1726/24/10/105017>. (Article)
- [31] Z. Chen, Y. Xia, J. He, Y. Xiong, G. Wang, Elastic-electro-mechanical modeling and analysis of piezoelectric metamaterial plate with a self-powered synchronized charge extraction circuit for vibration energy harvesting, *Mech. Syst. Signal Process.* 143 (2020) 106824. <https://doi.org/10.1016/j.ymssp.2020.106824>. (Article)
- [32] LTC3588-2 Datasheet and Product Info | Analog Devices, (n.d.). <https://www.analog.com/en/products/ltc3588-2.html> (accessed September 18, 2022).
- [33] F. B. Gurbuz, K. Kasyisli, S. Demirbas, R. Bayindir, I. Colak, M. Roscia, "Multi Input-Multi Output (MIMO) converter system fed by Wind Energy." 2022 11th International Conference on Renewable Energy Research and Application (ICRERA). IEEE, 2022. <https://doi.org/10.1109/ICRERA52334.2021.9598760>. (Article)
- [34] A. Brenes, A. Morel, D. Gibus, C.-S. Yoo, P. Gasnier, E. Lefeuvre, A. Badel, Large-bandwidth piezoelectric energy harvesting with frequency-tuning synchronized electric charge extraction, *Sens. Actuators Phys.* 302 (2020) 111759. <https://doi.org/10.1016/j.sna.2019.111759>. (Article)
- [35] Y. El Hmamsy, C. Ennawaoui, I. Najihi, A. Hajjaji, The Synchronized Electrical Charge Extraction Regulator for Harvesting Energy Using Piezoelectric Materials, in: S. Motahhir, B. Bossoufi (Eds.), *Digit. Technol. Appl.*, Springer International Publishing, Cham, 2021: pp. 1517–1527. https://doi.org/10.1007/978-3-030-73882-2_138. (Book Chapter)